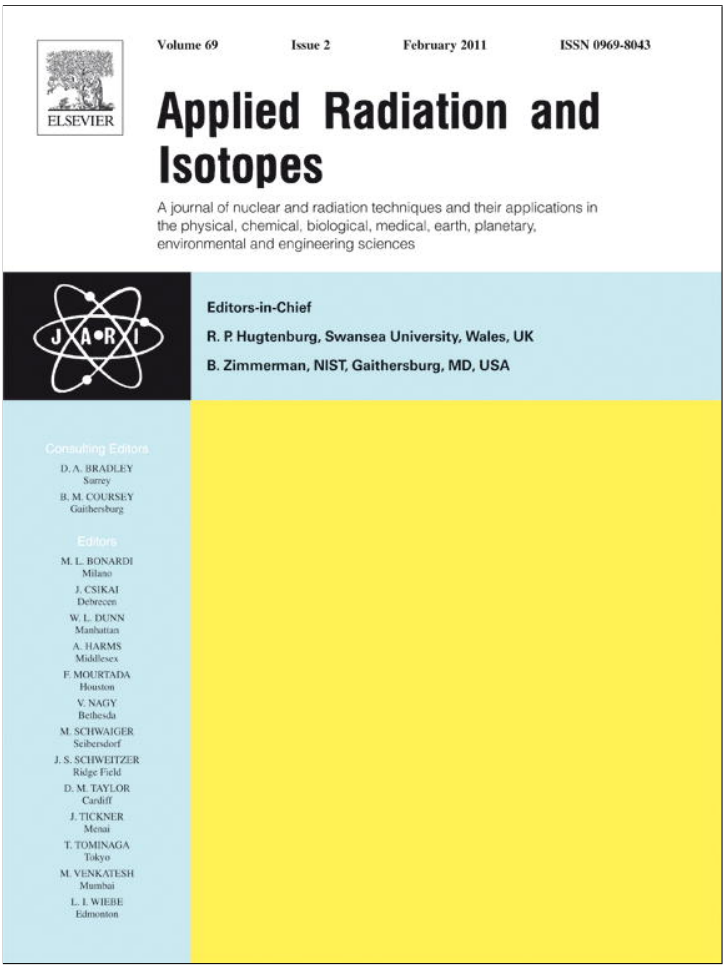

Applied Radiation and Isotopes 69 (2011) 320–326

Contents lists available at ScienceDirect

Applied Radiation and Isotopes

journal homepage: www.elsevier.com/locate/apradiso

No evidence for antineutrinos significantly influencing exponential β^+ decay

R.J. de Meijer [a,b,*], M. Blaauw [c], F.D. Smit [d]

[a] Stichting EARTH, de Weehorst, 9321 XS 2 Peize, The Netherlands
[b] Department of Physics, University of the Western Cape, Bellville, South Africa
[c] Reactor Institute Delft, Faculty of Applied Sciences, Delft University of Technology, Mekelweg 15, 2629 JB Delft, The Netherlands
[d] iThemba LABS, P.O. Box 722, Somerset West, 7129, South Africa

ARTICLE INFO

Article history:
Received 19 April 2010
Received in revised form
31 July 2010
Accepted 2 August 2010

Keywords:
Radioactivity
Beta decay
Decay constants
Solar neutrinos
Geoneutrinos
Reactor antineutrinos

ABSTRACT

High-precision measurements were conducted on the time evolution of gamma-ray count rates during reactor-on and reactor-off periods to investigate the possible influence of antineutrinos on nuclear decay. This experiment was triggered by a recent analysis (Jenkins et al., 2009) of long-term measurements suggesting a possible link to variations in nuclear decay rate and solar neutrino flux. The antineutrino flux during reactor-off periods is mainly due to geoneutrinos and four orders of magnitude lower than during reactor-on periods. No effects have been observed for the two branches in the decay of ^{152}Eu and the decay of ^{137}Cs, ^{54}Mn and ^{22}Na. The upper limit determined of the ratio $\Delta\lambda/\lambda$ for ^{22}Na is $(-1\pm2)\times10^{-4}$, and ^{54}Mn is $(-1\pm4)\times10^{-4}$. In comparison to the interpretation of Jenkins et al. our measurements do not show any such effect to at least two orders of magnitude less. Hence either the hypothesis of Jenkins et al. is not true or else one of two rather unlikely possibilities must also be true: either the effect of neutrinos on β^- decay differs considerably from the effect of antineutrinos on β^+ decay, or the effect of antineutrinos on β^+ decay must be identical to their effect on β^- and electron-capture decay.

1. Introduction

A number of papers have recently addressed oscillations in radioactive decay. These papers were triggered by oscillations seen superimposed on top of the exponential decay as observed in the count rate of γ-rays following β^- decay of ^{32}Si by Alburger et al. (1986) and of ^{226}Ra and progeny as well as γ-rays following β^- decay of ^{152}Eu (Siegert et al., 1998). The oscillations in the decay rate have a magnitude of the order of 10^{-3}, have an oscillation period of one year and extend over a period of several years.

Oscillations of a much shorter period (7 s) were observed in the electron capture of hydrogen-like $^{140}Pr^{59+}$ and $^{142}Pm^{60+}$ ions in a storage ring at GSI, Darmstadt (Litvinov et al., 2008). Jenkins and Fischbach (2009) showed a significant decrease in the count rate of γ-rays in the decay of ^{54}Mn by electron capture during, or prior to, solar flares at the end of December 2006. The reported effects are of the order of 10^{-4}. In another paper Jenkins et al. (2009) attribute the oscillations observed by Alburger et al. (1986) and Siegert et al. (1998) to variations in the solar-neutrino flux as a result of the annual three percent variations in Earth–Sun distance. Such flux variations are also put forward as the reason for the decrease in ^{54}Mn γ-ray count rate during solar flares.

A number of papers (Semkow et al., 2009; Norman et al., 2009) challenge the interpretation by Jenkins et al., and either explain the oscillations by temperature variations in the experimental set up (Semkow et al., 2009), or find no evidence for such oscillations (Norman et al., 2009) related to the variations in Earth–Sun distance. At PTB, the oscillations were explained by a discharge effect of the current measuring electronics (Siegert et al., 1998; Schrader, 2007, 2010) caused by a background resulting from radioactive decay via charged particles in the environment of the electronics, e.g. radon and thorium and their progenies. Experimentally the situation is therefore not yet clear.

For solar electron neutrinos, the flux at the Earth's surface is around 2×10^{10} cm^{-2} s^{-1} and is very hard to vary. The situation for antineutrinos is quite different. One expects that if the effect is present for neutrinos it should also be observable for antineutrinos. The flux of antineutrinos coming from radiogenic processes in the Earth is estimated to be about 10^6 cm^{-2} s^{-1}. However, anthropogenic antineutrino sources are available in the form of nuclear reactors. A 1 GW$_{th}$ reactor produces about 3×10^{19} fissions per second (one fission yields $\sim3\times10^{-11}$ J). If the fission of uranium is exclusively of ^{235}U (6 antineutrinos per fission), the antineutrino source has a strength of about 2×10^{20} s^{-1}. Ignoring flavour-oscillation effects, at a distance of about 280 m from the core the flux of antineutrinos is equivalent to the solar neutrino

* Corresponding author at: Stichting EARTH, de Weehorst, 9321 XS 2 Peize, The Netherlands. Tel.: +31 50 5016654.
E-mail addresses: demeijer@geoneutrino.nl, rmeijer@geoneutrino.nl (R.J. de Meijer).

0969-8043/$ - see front matter © 2010 Elsevier Ltd. All rights reserved.
doi:10.1016/j.apradiso.2010.08.002

flux, and four orders of magnitude more than the flux of geoneutrinos. Under such conditions between reactor-on and reactor-off, temperature effects on the source–detector distance (Semkow et al., 2009) should be irrelevant. Larger antineutrino fluxes can always be obtained at closer distances to the reactor.

Another option is to conduct measurements at a research reactor with smaller source strength but at a closer distance. In this paper we report on the first results of testing the hypothesis that antineutrinos affect the decay rate of nuclei decaying by β^+. The experiments were carried out at 8 m distance from the centre of the core of the 2 MW_{th} research reactor at the Reactor Institute Delft of Delft University of Technology, the Netherlands. The estimated antineutrino flux of $5\times10^{10}\,cm^{-2}\,s^{-1}$ is about twice the electron neutrino flux coming from the Sun at the Earth's surface.

One of the motivations for this experiment is that, if this effect would be as large as the one suggested by Jenkins et al., it could be used as a compact and inexpensive way to monitor the status and possibly even the composition of a nuclear power reactor. Antineutrino monitoring of nuclear reactors has been demonstrated by e.g. Bowden et al. (2007) and Bowden (2008) promoting the IAEA to adopt antineutrino monitoring as a tool to safeguard for nuclear reactors (IAEA, 2009).

2. Experimental set-up

The measurements were carried out at the Reactor Institute Delft with the CAFIA detector, placed in the experimental vault of the reactor at a distance of 8 m from the centre of the reactor core. Except for the top and the side not facing the reactor, the detector was surrounded by 10 cm of lead. CAFIA is a 33% HPGe detector, connected to an ORTEC 574 spectroscopy amplifier and supplied with high voltage by an ORTEC 495 power supply. The signals were digitised in a Northern NS 623 ADC and stored hourly in a PC. For dead-time correction purposes a 25 Hz pulse generator was fed to the preamplifier. Its pulses were shaped to mimic a detector pulse.

For investigating a possible effect of antineutrinos on the β^+-decay, the γ-ray transitions listed in Table 1, grouped by nucleus, were chosen. The choice was made, apart from availability, on the expectation that at the reactor, no effect is to be expected for β^--decay and electron capture (EC). Moreover the nucleus ^{152}Eu is rather unique as its decay contains not only EC+β^+-decay but also β^--decay. The ratio of the γ-ray transition count rates of these two decay modes should be less prone to systematic uncertainties than a comparison between count rates of γ-ray transitions from radionuclides, which differ in half-life.

All measurements were made with the sources placed on the detector end cap. One hour long measurements were made over a period of 200 h. At the beginning of this period the reactor was on.

Table 1
Transitions, γ-ray energies and half-life times used in the present work.

Transition	E_γ (keV)	$t_{1/2}$
^{22}Na(β^+)^{22}Ne	1275	2.6019 a
^{54}Mn(EC)^{54}Cr	835	312.2 d
^{137}Cs(β^-)^{137}Ba	662	30.17 a
^{152}Eu(EC+β^+)^{152}Sm	122	13.542 a
	245	
	964	
	1112	
	1408	
^{152}Eu(β^-)^{152}Gd	344	13.542 a
	799	
m_0c^2+^{22}Na	511	

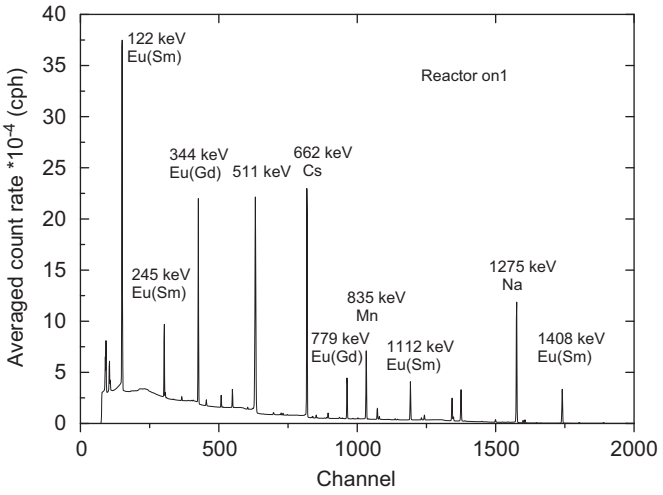

Fig. 1. Hourly gamma-ray spectrum averaged over reactor-on 1 period.

After 59 h the reactor was switched off for the weekend (65 h) and after the weekend the reactor was started up again and for the rest of the measuring time (76 h) remained on.

A truncated example of a γ-ray spectrum from the collection of sources is presented in Fig. 1. The pulser peak is situated near channel 3900 and is shown in Fig. 6. It shows the strength of the various γ-ray transitions relative to the continuum.

3. Analytical method

A measurement time of 200 h is far too short to determine a decay constant for a radionuclide with a half-life of the order of 1–10 years, even with count rates of 10^5–10^6 counts per hour. We therefore opted for a method based on observing changes in average count rate. The method follows straightforwardly from the laws of radioactive decay and is schematically presented in Fig. 2.

During the middle period with the reactor off, the literature value of decay constant λ applies, which will hereafter be referred to as regular decay. During reactor periods 1 and 3, the reactor is on and the decay constant becomes $\lambda+\Delta\lambda$. Count rates of gamma-rays are directly related to activities and will be indicated by A. For a given number of nuclei of a radionuclide, N_0, at $t=0$ the count rates will depend on the value of the decay constant: $A_0^\lambda\sim\lambda N_0$ and $A_0^{\lambda+\Delta\lambda}\sim(\lambda+\Delta\lambda)N_0$ so that $A_0^{\lambda+\Delta\lambda}=(1+(\Delta\lambda/\lambda))A_0^\lambda$. Note that for the same number of nuclei the initial count rate for decay constant $\lambda+\Delta\lambda$ is higher than for decay constant λ. If the source decays with decay constant λ (h^{-1}) or $\lambda+\Delta\lambda$, the count rate after t hours will be given by

$$A^\lambda(t)=A_0e^{-\lambda t}\quad\text{and}\quad A^{\lambda+\Delta\lambda}(t)=A_0e^{-(\lambda+\Delta\lambda)t},\quad\text{respectively}\qquad(1)$$

Here we note that the count rate for decay constant $\lambda+\Delta\lambda$ diminishes faster than for decay constant λ. This explains why in Fig. 2 the solid line starts higher but has a steeper slope. After some time the solid line will cross the dashed line. It also implies that more nuclei have decayed during the period with decay constant $\lambda+\Delta\lambda$ than would during regular decay. The number is relatively small and for practical reasons may be ignored, but to make the reader aware of this effect the solid line during period t_1, being the reactor-off period, will be slightly below the dashed line. The ratio of the two count rates of the solid lines in Fig. 2 at $t=t_0$ represents the change of decay constant for the same number of nuclei and corresponds to the factor $1+(\Delta\lambda/\lambda)$. When

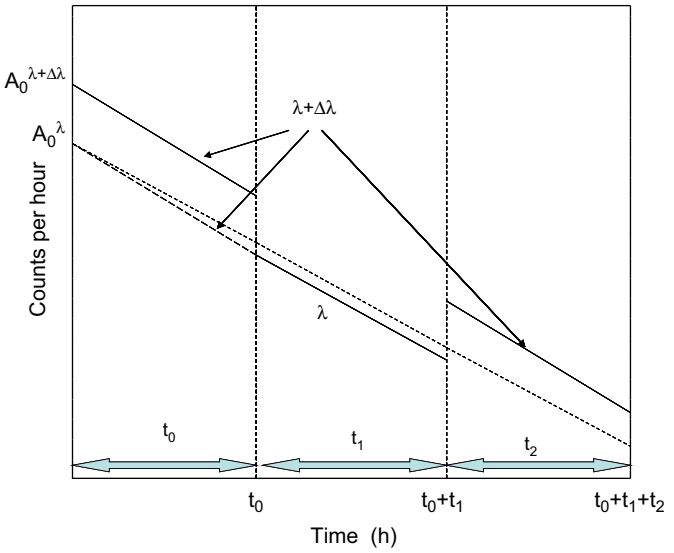

Fig. 2. Schematic diagram showing the count rates for decay constants λ and $\lambda+\Delta\lambda$ during the three reactor periods (on–off–on) if there were to be an effect.

the reactor is switched on again at $t=t_0+t_1$ the decay constant becomes $\lambda+\Delta\lambda$. Again the count rate increases by the same factor $1+(\Delta\lambda/\lambda)$ and the decay rate will be faster, similar to the situation in period reactor-on 1.

The total number of counts collected over a period of t_0 hours is given by:

$$n_{t_0}^{\lambda} = \int_0^{t_0} A^{\lambda}(t)dt \equiv \overline{A^{\lambda}}\, t_0 \tag{2}$$

The time-averaged hourly count rate $\overline{A^{\lambda}}$ in this equation is approximated by the (weighted) average of the count rates as observed in a series of measurements where the duration of each measurement (1 h) is very short compared to the half-life time of the radionuclide. For the present measurements three average values are deduced: $\overline{A_{on1}}$, $\overline{A_{off}}$ and $\overline{A_{on2}}$.

At $t=t_0$ the ratio of the count rates for the solid curves is given by

$$1+\frac{\Delta\lambda}{\lambda} = \frac{\overline{A_{on1}}\, e^{-(1/2)(\lambda+\Delta\lambda)t_0}}{\overline{A_{off}}\, e^{(1/2)\lambda t_1}} \tag{3}$$

Since Eq. (3) cannot be solved analytically, we introduce $x=1+(\Delta\lambda/\lambda)$, $a=A_{on1}/\overline{A_{off}}\, e^{(1/2)\lambda t_1}$ and $b=(1/2)\lambda t_0$. This leads to solving the equation

$$x = ae^{-bx} \tag{4}$$

Since bx is of the order of 10^{-3}, a series expansion is allowed leading to

$$x = a(1-bx) \quad \text{or} \quad x = \frac{a}{1+ab} = \frac{1}{b+\frac{1}{a}} \tag{5}$$

Propagation of uncertainties leads to

$\sigma(x)=(1/(b+(1/a))^2a^2)\,\sigma(a)=(1/(1+ab)^2)\sigma(a)\cong\sigma(a)$ since ab is of the order of 10^{-4}. Similarly

$$\sigma(\Delta\lambda)=\lambda\sigma(x)=\lambda\sigma(a) \tag{6}$$

with

$$\sigma(a) = \frac{\overline{A_{on1}}}{\overline{A_{off}}}\, e^{-(1/2)\lambda t_1}\sqrt{\left(\frac{\sigma(\overline{A_{on1}})}{\overline{A_{on1}}}\right)^2+\left(\frac{\sigma(\overline{A_{off}})}{\overline{A_{off}}}\right)^2} \tag{7}$$

For the reactor-on 2 period the value of $1+(\Delta\lambda/\lambda)$ can in a similar way as for the reactor-on 1 period, be derived from the values of $\overline{A_{off}}$, and $\overline{A_{on2}}$:

$$1+\frac{\Delta\lambda}{\lambda} = \frac{\overline{A_{on2}}\, e^{(1/2)(\lambda+\Delta\lambda)t_2}}{\overline{A_{off}}\, e^{-(1/2)\lambda t_1}} \tag{8}$$

which reduces to Eqs. (8) and (9) with $c=(\overline{A_{on2}}/\overline{A_{off}}\, e^{-(1/2)\lambda t_1})$, and $d=-\frac{1}{2}\lambda t_2$and

$$\sigma(c) = \frac{\overline{A_{on2}}}{\overline{A_{off}}}\, e^{\frac{1}{2}\lambda t_1}\sqrt{\left(\frac{\sigma(\overline{A_{on2}})}{\overline{A_{on2}}}\right)^2+\left(\frac{\sigma(\overline{A_{off}})}{\overline{A_{off}}}\right)^2} \tag{9}$$

4. Data analysis and results

Peak contents are often deduced by peak-fitting procedures. Peak integration is generally considered to be more straightforward than peak fitting, especially with respect to uncertainty estimation. For this reason we opted for peak integration. In peak integration the continuum part under the peak is estimated from the areas (regions of interest) to the high- and low-energy side of the peak. The net peak content is then obtained by subtracting the continuum part from the peak area.

Peak contents were derived from regions of interest denoted by below the peak energy (ROI-L), around the peak energy (ROI-P) and above the peak energy (ROI-H). These ROIs comprise m_L, m_P and m_H channels, respectively. The continuum under the peak, N_c, is estimated by

$$N_c = \frac{m_p}{2}\left(\frac{N_L}{m_L}+\frac{N_H}{m_H}\right) \tag{10a}$$

where N_L and N_H are the contents of ROI-L and ROI-H, respectively. The net number of counts N_p^{net} and its uncertainty ΔN_p^{net} are given by

$$N_p^{net} = N_P - N_c \tag{10b}$$

$$\Delta N_p^{net} = \sqrt{N_p+\left(\frac{m_p}{2}\right)^2\left(\frac{N_L}{m_L^2}+\frac{N_H}{m_H^2}\right)} \tag{10c}$$

In Eqs. (10b) and (10c) N_P represents the number of counts in ROI-P and Eq. (10c) is based on the assumption that the uncertainties in N_P, N_L and N_H equal the square root of their values. To allow for dead-time and pulse pile-up corrections, the set-up contains a pulse generator operating at a rate of 25($\pm 25\times10^{-6}$) Hz.

4.1. Background

It is well known that during reactor-on periods, activation of the air takes place in the reactor vault where one of the activation products is ^{41}Ar. The decay of ^{41}Ar produces a $E_\gamma=1294$ keV γ-ray. Fig. 3 shows the count rate of the $E_\gamma=1294$ keV line per hour over the entire period. One notices that during the reactor-off period the count rate is low and that during reactor-on periods strong oscillations occur with a diurnal oscillatory pattern. Fig. 4 shows the total count rate during the entire measuring period of 200 h. Firstly, one notices the high count rate of the spectra—about 6000 s^{-1}. Secondly, the oscillatory pattern, as observed for the $E_\gamma=1294$ keV line, also shows up in the total count rate, but the absolute magnitude of the oscillations is an order of magnitude larger than for the full-energy peak at $E_\gamma=1294$ keV. This is not a surprise in view of the contribution from the Compton events and the contribution by the electrons of the β^--decay. The oscillations are of the order of 1% of the total count rate. Thirdly, the total count rate seems to decrease with time. Fitting a decay function to the total count rate during the reactor-off period reveals a half-life

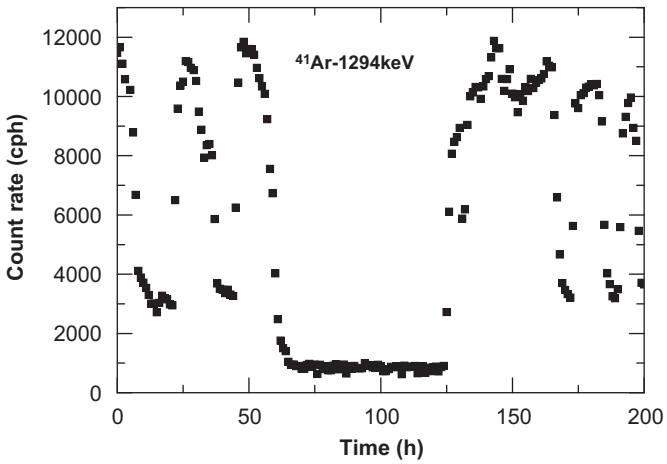

Fig. 3. Hourly count rate in the ^{41}Ar-decay peak at $E_\gamma = 1294$ keV.

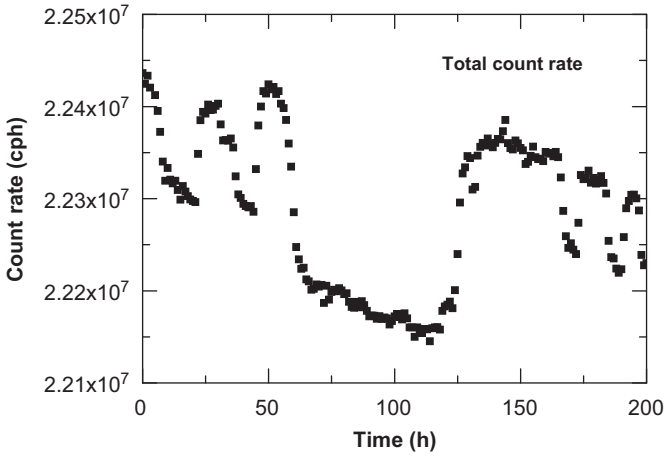

Fig. 4. Hourly total count rate.

of 1.54×10^4 h = 1.24 a. Qualitatively this value seems to be consistent with an interplay between the decay of ^{54}Mn and ^{22}Na.

Variations in the background should be part of the continuum under the peak and the method to determine the net peak area should remove these variations. One of the most stringent tests of the background removal procedure is the analysis of the $E_\gamma = 122$ keV line, because of its good statistics due to the high count rate and its wide ROIs due to the low-energy tail. The results are presented in Fig. 5. Except for the panel with the net counts, the three others clearly show the influence of the background variations. The fact that in the net-count panel the background variations are no longer visible supports the adopted procedure. In the net-count panel there are some noticeable steps at the transitions in reactor status. These steps are a likely indication of changes in dead time and/or pulse pile-up. The scatter in the data, however, is of a similar order as the effect that we are after.

4.2. Dead time and pulse pile-up

A pulse generator was included in the set-up to allow for dead time and pulse pile-up corrections. The peak of the pulser was positioned at the high-energy end of the spectrum. Fig. 6 shows a part of the high-energy side of the time-averaged γ-ray spectrum, containing the pulser peak. It also shows that the pulser peak has a tail extending to the high-energy end of the spectrum. The tail is formed by pulse pile-up that includes a small peak near channel 4060, which is the pulse pile-up reflection of the $E_\gamma = 122$ keV peak. Such a pile-up tail will be present at each peak in the spectrum, but will not be clearly noticeable because of the dominance of other continuum contributions such as Compton scattering, and the fact that the peaks have a low-energy tail. As we could not consistently analyse both the pulser peak and the γ-ray peaks in the spectrum in the same way, we abandoned this attempt to correct for dead time and pulse pile-up.

As indicated in Section 4.1 the background variations are well accounted for in the determination of the net count rates. The remaining effects of dead time and pulse pile-up, however, are of the same magnitude as the statistical variation in the data. To improve the statistics we will consider the weighted averages over each of the three reactor status periods. This implicitly

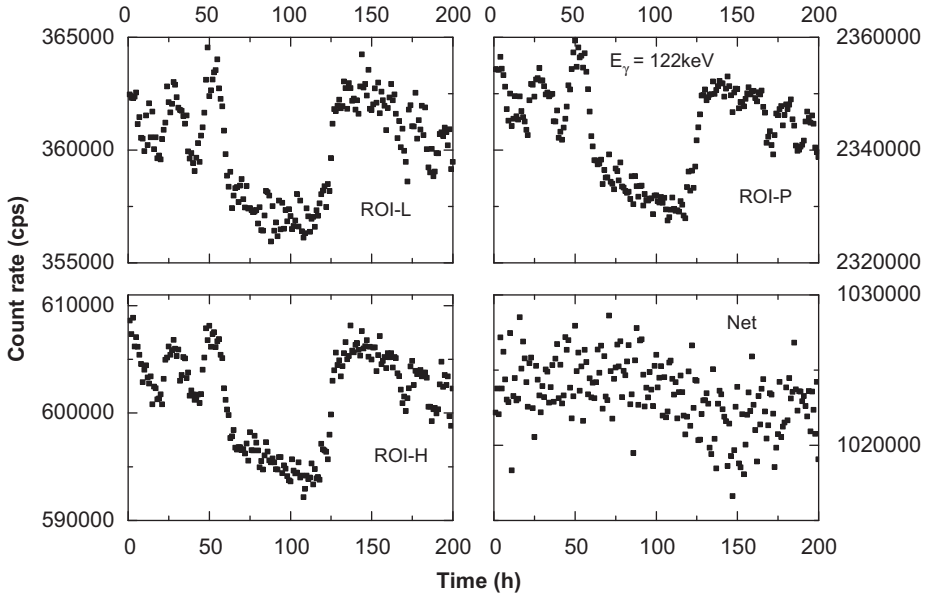

Fig. 5. Counts per hour measurement as a function of time for the three ROIs and the net peak content for the 122 keV line of Eu.

makes the assumption that the counts are normally distributed. A comparison between the weighted average and the average gives a difference of one count in more than half a million, and therefore the use of a weighted average is justified. The procedure of a weighted average has the advantage that a reduced χ^2-test may be carried out. The deviations from unity will also indicate to what extent the corrections for the oscillations have been successfully handled.

Below, the weighted averages per reactor period are derived for the transitions in the decay of ^{152}Eu and ^{137}Cs after the count rates have been corrected for decay. If the decay rates are correct, the only difference between the weighted averages will be the change in dead time and pulse pile-up. Table 2 presents an overview of the weighted averages of the net peak areas for transitions in the decay of ^{152}Eu to ^{152}Sm and ^{152}Gd for the three reactor periods. One notices that for each of the reactor periods the χ^2-values are close to unity, especially for the summed values. From these values there is no indication that within a reactor status period the actual decay rate differs significantly from the literature value. In the last row the dead time and the pulse pile-up corrections based on the Eu decay are presented.

The case of ^{152}Eu is particularly interesting since the decay to ^{152}Sm proceeds by EC and β^+, whereas the decay to ^{152}Gd is by β^-. If antineutrinos would influence the decay, one expects an effect for β^+-decay only. This makes the ratio of count rate of the two branches independent of dead-time and pulse pile-up effects. The ratio for the three reactor periods is given in Table 3.

The results in Table 3 indicate that there is no count rate ratio difference between reactor-on and reactor-off. Within an overall relative uncertainty of 1.6×10^{-4} the value is constant. In the ^{137}Cs hourly count rate, the change was found to be consistent with regular decay and hence ^{152}Eu and ^{137}Cs were used to establish the relative change in the dead-time and pulse-pile-up factor for the two reactor-on periods relative to the reactor-off periods.

The results are presented in Table 4. As the results are decay corrected, the ratios off/on are indications of the dead-time and pulse pile-up corrections, which can be seen to be relatively small ($<2\times10^{-3}$) and that within the statistical uncertainties the correction factors remain unchanged after inclusion of the Cs data. Somewhat disturbing is the fact that the corrections for reactor-on 2 are larger than for reactor-on 1. This result is contrary to the expectation, as during reactor-on 1 the average count rate is higher than during the reactor-on 2 period, as can be seen in Fig. 4. We have been through the analyses carefully several times and we could not find anything in our experiment that could cause this. In this assessment we noticed that the averages of the total count rate during reactor-on 1, -off and –on 2 are 2.236×10^7, 2.218×10^7 and 2.232×10^7 cph, respectively. The difference in total count rate between the two reactor-on periods seems too small for dead time to cause the difference in the off/on ratios in Table 4. The difference in the ratios may rather be related to the difference in the shape of the room background spectrum and the "source" spectrum. The background spectrum has a relatively stronger continuum component at low energies, in comparison to the source spectrum.

Pulse-pile-up for the lines in the source spectrum will not occur in the ROI-L, but mainly in ROI-H and to a lesser extent in ROI-P (see Fig. 6). So pulse-pile-up is likely to affect the net count rate and is dependent on the relative intensity of background to source spectra. Fig. 4 indicates that during reactor-on 2 the

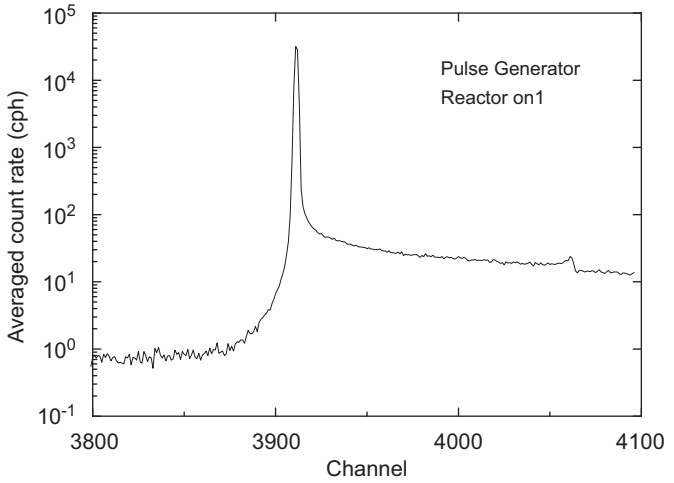

Fig. 6. Hourly count rate near the pulse generator peak averaged over the reactor-on 1 period.

Table 3
Ratio of the count rates for transitions in the decay of ^{152}Eu to ^{152}Sm and ^{152}Gd for the three reactor periods and the average value.

Reactor status	Count-rate ratio ^{152}Sm/^{152}Gd
On1	2.7412 (0.0008)
Off	2.7410 (0.0008)
On2	2.7408 (0.0007)
Average	2.7410 (0.0004)

Table 2
Averaged net peak areas, their uncertainties and the corresponding χ^2-values for transitions following the decay of ^{152}Eu to ^{152}Sm and ^{152}Gd in spectra measured for 1 h periods with the reactor-on and reactor-off. The values are derived under the assumption that the status of the reactor was inconsequential to the spectra. Values have not been corrected for dead time but have been corrected for nuclear decay.

Transition	E_γ (keV)	Mean	Unc.	χ^2	Mean	Unc.	χ^2	Mean	Unc.	χ^2
		Reactor-on 1			**Reactor-off**			**Reactor-on 2**		
^{152}Eu(EC+β^+)^{152}Sm	122	1,024,500	300	0.87	1,024,800	300	0.77	1,022,900	200	1.14
	245	172,120	90	0.70	171,840	90	1.14	171,880	80	1.01
	964	103,380	60	0.89	103,470	50	0.96	103,350	50	0.83
	1112	90,210	50	1.25	90,340	50	1.18	90,160	40	1.34
	1408	110,030	50	1.13	110,160	40	0.80	110,020	40	0.87
Sum		*1,500,200*	*300*	*0.86*	*1,500,600*	*300*	*0.68*	*1,498,300*	*300*	*0.94*
^{152}Eu(β^-)^{152}Gd	344	440,000	100	1.18	440,070	100	1.78	439,480	90	0.96
	799	107,290	60	0.95	107,400	50	1.11	107,200	50	1.12
Sum		*547,300*	*120*	*1.13*	*547,460*	*100*	*1.78*	*546,680*	*140*	*0.94*
Overall Sum		**2,047,500**	**300**	**0.87**	**2,048,000**	**300**	**0.90**	**2,045,000**	**300**	**0.89**
Dead-time correction		*1.00024*	*20*					*1.00147*	*20*	

Table 4
Averaged hourly count rates for β^- emitters ^{152}Eu, ^{137}Cs, corrected for decay, their sum and the ratio off/on for the three reactor periods.

Reactor status	^{152}Eu	^{137}Cs	^{152}Eu+^{137}Cs	Ratio off/on
On1	2,047,500(300)	604,360(120)	2,651,900(300)	1.00023(0.00017)
Off	2,048,000(300)	604,490(110)	2,652,500(300)	
On2	2,045,000(300)	603,190(103)	2,648,200(300)	1.00163(0.00016)

Table 5
Time-averaged hourly count rate, corrected for relative dead time and pulse pile-up, and relative changes in the decay constants for ^{22}Na and ^{54}Mn.

Reactor status	$\overline{A(^{22}Na)}$	$\Delta\lambda/\lambda$ (^{22}Na)	$\overline{A(^{54}Mn)}$	$\Delta\lambda/\lambda$ (^{54}Mn)
On1	353,430(100)	$(-3\pm4)\times10^{-4}$	195,781(80)	$(4\pm5)\times10^{-4}$
Off	352,880(80)		194,611(70)	
On2	352,150(90)	$(1\pm3)\times10^{-4}$	193,228(70)	$(-6\pm5)\times10^{-4}$
Average		$(-1\pm2)\times10^{-4}$		$(-1\pm4)\times10^{-4}$

background contribution is larger than in reactor-on 1 and hence one expects a somewhat larger pulse-pile up correction. This would also explain why in Fig. 5 the net count rate shows a slight dip during reactor-on 2. The above also explains qualitatively why we could not use the pulser peak for dead time and pulse-pile-up correction, as discussed in the beginning of this section.

By taking the off/on ratios of Table 4 as correction factors of dead time and pulse pile-up, their effects on gamma-ray spectra for the sources is assumed to be compensated.

4.3. Results for ^{22}Na and ^{54}Mn

Together with the relative correction factors for dead time and pulse pile-up, the equations presented in Section 3 can be used to determine the relative change in decay constant due to the changes in antineutrino flux. Table 5 lists the time-averaged hourly count rates, corrected for the relative corrections for dead time and pulse pile-up and the resulting relative changes in decay constant due to the presence of an antineutrino source. From Table 5 one notices that for both ^{22}Na and ^{54}Mn, within the statistical uncertainties, the values for $\Delta\lambda/\lambda$ are the same. Therefore within the precision of this measurement we can state that, if antineutrinos affect β-decay at all, the effect on the decay rate due to the presence of an antineutrino source is the same for β^+-decay, β^--decay and electron capture. There is also no indication that such a hypothetical effect depends on the properties of the radionuclides involved (^{22}Na, ^{54}Mn, ^{137}Cs and ^{152}Eu). Moreover the values are consistent with a dominance of statistical over systematic uncertainties. This supports the approach of making relative corrections for dead time and pulse pile-up.

Finally we would like to point out that this upper limit of a possible effect of antineutrinos on the decay of ^{22}Na or ^{54}Mn agrees very well with the upper limit deduced from the decay of ^{152}Eu into ^{152}Sm and ^{152}Gd. The values for the ratios of these two decay branches of ^{152}Eu are independent of the dead time and pulse pile-up corrections. Again this agreement supports our conclusion.

5. Discussion and conclusions

Jenkins et al. suggested as an explanation for annual oscillations in the decay curve of ^{32}Si, the influence of electron neutrinos on β^--decay. In the present paper we have opted to test this suggestion by examining possible changes in decay constant of β^+-decay under the influence of electron antineutrinos. We carried out the experiment at a similar antineutrino flux as the solar flux at the Earth's surface. To obtain good statistics and reduce influences from background we allowed high count rates, despite the potential uncertainties due to dead time and pulse pile-up. In this paper we have assumed that dead time and pulse pile-up can be corrected for by comparing the decay corrected count rates of γ-rays emitted in the β^--decay of ^{152}Eu and ^{137}Cs. The results support our assumption.

The present series of high count rate experiments near the research reactor at Delft University of Technology has yielded no indication for a change in decay constant for ^{22}Na and ^{54}Mn. An upper limit for such an effect can be set at a few times 10^{-4}. The flux of antineutrinos at a distance of 8 m from the reactor core of this 2 MW_{th} reactor is estimated to be about 5×10^{10} cm^{-2} s^{-1} during reactor-on and about 10^6 cm^2 s^{-1} during reactor off periods. This flux with the reactor on is about twice the electron neutrino flux from the Sun.

Jenkins et al. argue that the 0.3% oscillations observed in the decay of ^{32}Si, reported by Alburger, are due to a change in the solar electron neutrino flux of 6% (1.2×10^9 cm^2 s^{-1} at a flux of 2×10^{10} cm^2 s^{-1}). In the present experiment the antineutrino flux changed nearly 100% (from 10^6 to 5×10^{10} cm^2 s^{-1}). One would therefore expect a 16 times bigger effect in the decay-rate oscillations, if the interpretation of Jenkins et al. (2009) were to be correct. Our result of limiting any possible effect to $<3\times10^{-4}$, is a factor of about 400 lower than would be expected, under the assumptions that the influence of electron antineutrinos on β^+-decay is the same as for electron neutrinos on β^--decay and the effect being proportional to the flux. This limit also holds if we assume that the influence of antineutrinos on β^+-decay and β^--decay is the same. Hence either the hypothesis of Jenkins et al. is not true or the effect of neutrinos on β^--decay differs considerably from the effect of antineutrinos on β^+-decay.

One of the motivations for carrying out the present experiment was to investigate if a continuous measurement of the count rate due to the decay of, e.g. ^{22}Na could be used to monitor a nuclear power plant with respect to its operation and/or to changes in its fuel composition (Bowden et al., 2007; Bowden, 2008). The antineutrino flux at a distance of about 20 m from a 1 GW_{th} reactor will be about 4×10^{12} cm^{-2} s^{-1}, two orders of magnitude higher than in the present experiment. Again assuming a linear dependence on antineutrino flux, the upper limit deduced from the present experiment, could still correspond to a 3% change in decay constant. Such an effect could well be measurable and one may even expect that changes in fuel composition could be detected in this way at a distance of 20 m. Such a measurement would therefore still be worthwhile.

The present experiment has taught us the pitfalls of a high-count rate experiment in the vicinity of a reactor. We anticipate utilising this experience to repeat this type of experiment near a 3 GW_{th} power reactor.

Acknowledgements

This investigation was part of the research programme of Stichting EARTH. One of us (RdM) likes to thank the Reactor Institute Delft for their hospitality and cooperation to facilitate this experiment. The authors would like to thank the two anonymous reviewers for their careful and constructive contributions to the paper.

References

Alburger, D.E., Harbottle, G., Norton, E.F., 1986. Half-life of ^{32}Si. Earth and Planetary Science Letters 78, 168–176.

Bowden, N.S., et al., 2007. Experimental results from an antineutrino detector for cooperative monitoring of nuclear reactors. Nuclear Instruments and Methods A572, 985–998.

Bowden, N.S., 2008. Reactor monitoring and safeguards using antineutrino detectors. Journal of Physics: Conference Series 136, 022008.

Jenkins, J.H., et al., 2009. Evidence for correlations between nuclear decay rates and Earth–Sun distance. Astroparticle Physics 32, 42–46.

Jenkins, J.H., Fischbach, E., 2009. Perturbation of nuclear decay rates during the solar flare of 13 December 2006. Astroparticle Physics 31, 407–411.

IAEA, 2009. Final report: Focused Workshop on Antineutrino Detection for Safeguards Applications. IAEA STR-361.

Litvinov, Y.A., et al., 2008. Observation of non-exponential orbital electron capture decays of hydrogen-like ^{140}Pr and ^{142}Pm ions. Physics Letters B664, 162–168.

Norman, E.B., et al., 2009. Evidence against correlations between nuclear decay rates and Earth–Sun distance. Astroparticle Physics 31, 135–137.

Schrader, H., 2007. Ionization chambers. Metrologica 44, 53–66.

Schrader, H., 2010. Half-life measurements of long-lived radionuclides—new data analysis and systematic effects. Applied Radiations and Isotopes 68, 1583–1590.

Semkow, T.M., et al., 2009. Oscillations in radioactive exponential decay. Physics Letters B675, 415–419.

Siegert, H., Schrader, H., Schotzig, U., 1998. Half-life measurements of Europium radionuclides and the long term stability of detectors. Applied Radiations and Isotopes 49, 1397–1401.